International Journal of Engineering & Technology, 7 (4.22) (2018) 42-48

International Journal of Engineering & Technology

Website: www.sciencepubco.com/index.php/IJET

Research paper

Determination of CCT Due to Interconnected link Tripping using the OMIB and EAC

Nur Ashida Salim[1], *, Jasronita Jasni[2], Norfishah Ab Wahab[1], Nur Fadilah Ab Aziz[3], Nur Azzammudin Rahmat[3] Zuhaila Mat Yasin[1], Hasmaini Mohamad[1]

[1] Faculty of Electrical Engineering, Universiti Teknologi MARA, 40450 Shah Alam, Selangor, Malaysia
[2]Centre for Electromagnetic and Lightning Protection Research (CELP), Department of Electrical and Electronic Engineering, Faculty of Engineering, Universiti Putra Malaysia, 43400 Serdang, Selangor, Malaysia
[3]Institute of Power Engineering, Electrical Power Department, College of Engineering, Universiti Tenaga Nasional, Malaysia
**Corresponding author E-mail: nurashida606@salam.uitm.edu.my*

Abstract

This paper presents an algorithm to determine the critical clearing time (CCT) due to the effect of interconnected link tripping by applying the one machine infinite bus (OMIB) equivalent system method and equal area criterion (EAC). This paper also proposes the implementation of graphical user interface (GUI) to monitor and predict the CCT from time to time. The CCT is defined as the highest time interval by which the fault is expected to be cleared with the aim of maintaining the electricity supply stability. The computation of important numerical development of CCT is deduced from the entails three fault situations, which are; pre-fault, during fault and post-fault situations, with the main focus on pre-fault situation. The CCT becomes significantly shorter whilst transient instability is induced by a three-phase fault occurred at the bus bar next to the substation connected with a sensitive generator. It is sufficient to maintain the transient stability albeit fault occurred at other locations by setting the protection relay with the computed value of CCT. A circuit breaker which is installed and operated before the smallest CCT will not affect the transient instability throughout the occasion of fault. The IEEE Reliability Test System 1979 (IEEE RTS-79) is used to verify the accuracy of the proposed methodology in determining the CCT.

Keywords: *critical clearing time; critical clearing angle; equal area criterion; dynamic system sequence of fault; transient stability assessment; one machine infinite bus.*

1. Introduction

In this modern era with full of technology, the usage of electricity is very wide and electricity now is very important for people in this world. But the most important use of electricity is to the industry because of the business that they run where they are producing products to make people's life become easier. So, it is very important to maintain the stability of an electricity supply and to avert any unwanted event happen such as breakdown or blackout that can make the whole system stop running. After having some form of distraction, it still able to return to normal or stable operating situations and that is the meaning of stability in a electricity supply. Besides that, stability also means the ability to maintain a electricity supply and avert any breakdown or blackout or sequence of fault by providing precautionary action[1]. Equally, instability is a situation representing falling out of step or loss of synchronism[2]. In addition, stability also means the propensity of a electricity supply to create restoring forces equal to or greater than the distracting forces in order to maintain the state of equilibrium. The system is said to remain stable-state (to stay in synchronism), if the forces propensity to hold machines in synchronism with one another are enough to overcome the distracting forces. Stability is the process at planning level when new generating and transmitting facilities are developed. The studies are needed in determining the relaying system, critical fault clearing time of interconnected link and critical clearing angle between the system[3]. The generator will no longer work at synchronous speed and lose it synchronization because of the electricity supply. This will conduct to voltage, current and power to oscillate extremely. Due to this situation, it could cause damage to the loads which obtain electric supply from the unbalanced system.

Intricacy of planning and operating a contemporary electricity supply is consistently escalating due to less power reserves, complex interface amongst various system controllers, more intricate coordination, superior interdependence among interconnected systems and large power transfers over long distance of interconnected link . High demands that have forced the system to be managed closer to their dynamic security limits can cause instability of a system and become a main pressure for system operation. This can be proven by the recent increase in electricity supply blackouts [4]. Typically, a big impact to the society and economy of the country is cause from the breakdown or sequence of fault or large area blackout of a electricity supply. Even serious consequences also can happen from short interruptions in electrical supply. For that reason, it is important to pursue for a clarification that provides precautionary action so that it could be applied in order to avert from incidence of a sequence of fault in electricity supply [5]. Responsibility for safe service of electricity supply is important for transient stability assessment (TSA). The effects of the system due to instability for instance line switching, loss of generators or demand and also fault is examined by taking into account through the transient stability [6]. An electricity supply is transiently stable for a particular steady-state operating situation and for a particular big distraction if, subsequent that distraction; it reaches an acceptable steady-state operating situation [4].

To date, in order to provide precautionary action, according to the literature review on the study of transient stability assessment in the determination of accurate value of CCT, there are several methods have been developed and discussed. For example, direct method and hybrid method. Both of this method usually used in transient stability studies. Direct method also has several types such as potential energy boundary surface method [7], boundary of stability region based controlling unstable equilibrium point method [8] and EAC [9]. On top of that, the direct method provides a stability index which gives stability margin of an operating point in terms of energy stored in the system [10]. Next, the hybrid method of transient stability assessment takes opportunity of Lyapuno's type energy function and merge it with the normal time domain simulation technique. In most cases, the hybrid transient stability assessment technique identifies some stability index value where it will give impact to the security status of electricity supply. According to the research that has been made by [11], for fast computation of CCT for transient stability assessment, the authors proposed a normalized energy function approach, where it normalizes the inertia by using an average centre angle instead of centre of inertia.

According to the research that has been done through the literature review, it is obligation to investigate the CCT due to its considerable effect to an electricity supply operation such as force tripping and load increase. Furthermore, electricity supply has a non-linear dynamic behavior with multi-inputs and multi-outputs variables, which makes its analysis not straight forward. For that reason, one of the best proposition techniques to discover the CCT is by using OMIB equivalent method. The IEEE RTS-79 system is used as the case study to confirm the achievement of the proposed method considered in the analysis of CCT. Multi-machine system to a single machine equivalent transient stability system of an electricity supply is part of planning and operation planning studies where it emphasizes on the ability of a system to resist severe interruption whilst ensuring continuity of service. The advantage of this technique is a multi-machine system can be reduced by simplifying the original large-scale system to a dynamic equivalent model. This kind of technique of OMIB model can obtain the simplest dynamic equivalent model of a multi-machine system. Once a multi-machine system is represented by the OMIB equivalent model, its change can be used to identify the transient stability situation of the system.

2. Methodology

Critical machine (cm) and non-critical machine (ncm) can be identified by the transient stability limit as defined in (1). Only several machines are recognized as the critical apportioned machines for a given distraction on a huge system. Through the dynamic response of the severely disturbed machines, the stability of the entire system can also be proved. Equation (1a) and (1b)[12], is the difference between relative rotor angles regarding to the centre of inertia and the valuation of transient stability. The machine is said to be seriously unstable, cm, if the angle deviation, Δδn (t), exceeds 180o and vice-versa for the non-critical machine, ncm [13].

$$ncm = \Delta\delta_n\ (t) \leq 180^\circ \quad (1)$$
$$cm = \Delta\delta_n\ (t) \geq 180^\circ$$

Where,

$$\Delta\delta_n\ (t) = |\ \Delta\delta_n\ (t) - \delta_{COI}\ (t)| \quad (1a)$$

$$\delta_{COI}\ (t) = \left(\sum_{n=1}^{G} H_n\right)^{-1} \left(\sum_{n=1}^{G} H_n \delta_n\ (t)\right) \quad (1b)$$

Next, the rotor angle of OMIB is created according to the two identical rotor angles of δcm (t) and δncm (t) transformed from two rotor angle group of critical and non-critical machines, respectively. Hence, from (2)[9], the basic development of rotor angle of OMIB can be achieved.

$$\delta_{OMIB}(t) = \delta_{cm}(t) - \delta_{ncm}(t) \quad (2)$$

Where,

$$\delta_{cm}(t) = \frac{1}{M_{cm}} \sum_{n=cm} M_n \delta_n\ (t) \quad (2a)$$

$$\delta_{ncm}(t) = \frac{1}{M_{ncm}} \sum_{n=ncm} M_n \delta_n\ (t) \quad (2b)$$

M_{cm} : total inertia coefficient ofcm given by $\sum \pi\epsilon cm\ M_n$

M_{ncm} : total inertia coefficient of cm given by $\sum \pi\epsilon ncm\ M_n$

M : OMIB inertia coefficient defined by $2 \times H$

Nevertheless, due to its difficulty in calculating the generator real output power, $P_{\delta n}$ because of involving of large matrix size of n × k at every time gap compulsory by $\delta_n(t)$ in (2a) and (2b), the basic development of $\delta_{OMIB}\ (t)$ in (2) will not be used in the subsequent analysis. For that reason, utilizing (2) to compute the basic development of $\delta_{OMIB\ (t)}$ may yield to a computational load happened in the subsequent analysis. By using a simplified development of δ_{OMIB}, this predicament can be solved and resulting to a less calculation time which will be explained in the subsequent step.

The rotor angle of one machine infinite bus, $\delta_{OMIB\ (t)}$ must be computed at each time distance that is in the occurrence of pre-fault, during fault and post-fault situations. The evaluation of $\delta_{OMIB\ (t)}$ starts with the primary development of OMIB flow or swing given by (3) [14].

$$\frac{d^2\delta_{OMIB}}{dt^2} = \pi f_{rated} M^{-1}(P_{m_{OMIB}} - P_{e_{OMIB}}) \quad (3)$$

where,

OMIB mechanical input power, $P_{m_{OMIB}}$ (3a)

$$= \left(\frac{M_{cm}\, M_{ncm}}{M_{cm} + M_{ncm}}\right)\left[\left(\frac{1}{M_{cm}}\right)\left(\sum_{\pi\epsilon cm} P_{m_\pi}\right) - \left(\frac{1}{M_{ncm}}\right)\left(\sum_{\pi\epsilon ncm} P_{m_\pi}\right)\right]$$

OMIB mechanical input power, $P_{e_{OMIB}}$ (3b)

$$= \left(\frac{M_{cm}\, M_{ncm}}{M_{cm} + M_{ncm}}\right)\left[\left(\frac{1}{M_{cm}}\right)\left(\sum_{\pi\epsilon cm} P_{e_\pi}\right) - \left(\frac{1}{M_{ncm}}\right)\left(\sum_{\pi\epsilon ncm} P_{e_\pi}\right)\right]$$

Farther derivation of (3) will unravel to a basic development of OMIB flow or swing equation that is given by (4).

$$\frac{d^2\delta_{OMIB}}{dt^2} = \pi f_{rated} M^{-1}\left[P_{m_{OMIB}} - \left[P_{c_{OMIB}} + P_{max_{OMIB}} \sin(\delta_{OMIB} - v)\right]\right] \quad (4)$$

Where,

$$P_{m_{OMIB}} = \frac{M_{ncm} \sum_{n\epsilon cm} P_{m_{cm}} - M_{ncm} \sum_{n\epsilon ncm} P_{m_{ncm}}}{M_{cm} + M_{ncm}} \quad (4a)$$

$$P_{c_{OMIB}} = \frac{\left(M_{ncm} E'^{\,2}_{cm} G_{cm,cm}\right) - M_{cm}\left(\sum_{n\epsilon ncm} E'^{\,2}_{ncm} G_{ncm,ncm}\right)}{M_{cm} + M_{ncm}} \quad (4b)$$

$$P_{max_{OMIB}} = \sqrt{(C^2 + D^2)} \quad (4c)$$

$$v = -\tan^{-1}\left(\frac{C}{D}\right) \quad (4d)$$

$$C = \frac{(M_{cm} - M_{ncm}) \sum_{n\epsilon ncm} (E'_{cm})(E'_{ncm}) G_{cm,ncm}}{M_{cm} + M_{ncm}} \quad (4e)$$

$$D = \sum_{n\,\epsilon\, ncm} E'_{cm} E'_{ncm} G_{cm,ncm} \quad (4f)$$

The value of E' and G which is the shunt conductance of Y^{new}_{nk} entailed with (4b), (4e) and (4f). The value of P_m is required in the (4a). These has been explained in detailed in [15]. At every time distance of the three fault situations δ_{OMIB} is computed and this will be deliberated in the next explanation.

Basically, only a portion of swing equation in (4) is used to identify the rotor angle of OMIB at every time distance, δ_{OMIB+1} , of pre-fault, during fault and post-fault situations. In additions, in (4), referring to the changes in G at pre-fault, during fault and post-fault situations, $P_{e_{OMIB}}$, $P_{max_{OMIB}}$ and v are diverse. Then, the value of E' is permanent during all the three fault situations. Farther more, equation (4) also using a permanent value of $P_{m_{OMIB}}$ according to the P_m identified at the three situations of fault.

Starts with a derivation of (4) yielding to (5) and (6), an entire swing equation of δ_{OMIB+1} could be achieved.

$$\frac{d\delta_{OMIB}}{dt} = \Delta\omega_{OMIB} \quad (5)$$

$$\frac{d\Delta\omega_{OMIB}}{dt} = \pi f_{rated} M^{-1}\Big[P_{m_{OMIB}} - \Big[P_{c_{OMIB}} + P_{max_{OMIB}} \sin(\delta_{OMIB} - v)\Big]\Big] \quad (6)$$

By concentrating the event of throughout fault and post-fault situations, equation (6) is then describe by equations (7) and (8), respectively.

$$\left.\frac{d\Delta\omega_{OMIB}}{dt}\right|_{\delta_{OMIB,s}} = \pi f_{rated} M^{-1}\left[P_{m_{OMIB}} - \left(P^{df}_{c_{OMIB}} + P^{df}_{max_{OMIB}} \sin\left(\delta_{OMIB,s} - v^{df}\right)\right)\right] \quad (7)$$

$$\left.\frac{d\Delta\omega_{OMIB}}{dt}\right|_{\delta_{OMIB,s}} = \pi f_{rated} M^{-1}\left[P_{m_{OMIB}} - \left(P^{pf}_{c_{OMIB}} + P^{pf}_{max_{OMIB}} \sin\left(\delta_{OMIB,s} - v^{pf}\right)\right)\right] \quad (8)$$

Basically, to get the value of $\Delta\omega_{OMIB,s+1}$ and $\delta_{OMIB,s+1}$ throughout the pre-fault situation, δ^0_{OMIB} identified by equation (9) and $\Delta\omega^0_{OMIB,s} = 0$ are used in (6), (10), (11) and (12). $P_{c_{OMIB}}$, $P_{max_{OMIB}}$ and v are computed by concentrating the G bring out from given in [15], in (6). For that reason, the faulted bus and faulted line will not be eliminated from the creation of matrix. Equation (6) also needs the value of E'. At the pre-fault situation, the calculation of δ^0_{OMIB} and $P_{m_{OMIB}}$ need the values of Pm and δ^0_n. The achieved value of E' and $P_{m_{OMIB}}$ will be used respectively for calculating the $\delta_{OMIB,s+1}$ at every time gap during fault and post-fault situations.

$$\delta^0_{OMIB} = sin^{-1}\frac{P_{m_{OMIB}}}{P_{max_{OMIB}}} \quad (9)$$

At the pre-fault situation, in equations (7), (10), (11) and (12), the $\Delta\omega_{OMIB,s+1}$ and $\delta_{OMIB,s+1}$ are then used as the primary parameters to compute the value of $\Delta\omega_{OMIB,s+1}$ and $\delta_{OMIB,s+1}$ for the repeated time intervals during fault situation. In equation (7) including of $P^{df}_{c_{OMIB}}$, $P^{df}_{max_{OMIB}}$ and v^{df} are computed by concentrating the G bring out from Y^{new} during the event of fault. In the same way, the above-mentioned process is recurrent to determine the $\Delta\omega_{OMIB,s+1}$ and $\delta_{OMIB,s+1}$ at every time gap of post-fault situation using equations (8), (10), (11) and (12) which need the $\Delta\omega_{OMIB,s+1}$ and $\delta_{OMIB,s+1}$ computed at the last gap during fault situation. Equation (8) is computed according to the G created from the transient stability valuation that considers the elimination of faulted line with regards to the post-fault situation.

$$\Delta\omega_{OMIB,s+1} = \Delta\omega_{OMIB,s} + \left.\frac{d\Delta\omega_{OMIB}}{dt}\right|_{\delta_{OMIB,s}} \Delta t \quad (10)$$

$$\left.\frac{d\delta_{OMIB}}{dt}\right|_{\Delta\omega_{OMIB,s+1}} = \Delta\omega_{OMIB,s+1} \quad (11)$$

$$\delta_{OMIB,s+1} = \delta_{OMIB,s} + \left.\frac{d\delta_{OMIB}}{dt}\right|_{\Delta\omega_{OMIB,s+1}} \Delta t \quad (12)$$

Equations (10) and (12) are replaced with equations (13) and (14) using the modified Euler's method respectively, so that the specific results of $\Delta\omega_{OMIB,s+1}$ and $\delta_{OMIB,s+1}$ with fewer error could be achieved. Similarly, at the pre-fault, during fault and post-fault situations, the above-mentioned process can be used to identify the $\Delta\omega_{OMIB,s+1}$ and $\delta_{OMIB,s+1}$.

$$\Delta\omega_{OMIB,s+1} = \Delta\omega_{OMIB,s} + \left(\frac{\left.\frac{d\Delta\omega_{OMIB}}{dt}\right|_{\delta_{OMIB,s}} + \left.\frac{d\Delta\omega_{OMIB}}{dt}\right|_{\delta_{OMIB,s+1}}}{2} \right) \Delta t \tag{13}$$

$$\delta_{OMIB,s+1} = \delta_{OMIB,s} + \left(\frac{\left.\frac{d\delta_{OMIB}}{dt}\right|_{\Delta\omega_{OMIB,s}} + \left.\frac{d\delta_{OMIB}}{dt}\right|_{\Delta\omega_{OMIB,s+1}}}{2} \right) \Delta t \tag{14}$$

By substituting s+1 with t, thus $\delta_{OMIB,s+1}$ is finally well-defined as $\delta_{OMIB}(t)$. Hence, between the duration of t = 0 and $t = t_c$ followed by $t = t_c$ and $t = t_f$, the dynamic response $\delta_{OMIB}(t)$ of can be drawn. Whereby t_c is the CCT interval and t_f is the final simulation time. The network protection system should be operated within this critical time interval so that the faulty line or generator can be disconnect without causing any loss of generator synchronism. In the subsequent section the OMIB rotor angle obtained in equation (9) will be used in the determination of CCT for one machine system.

The transformation from multi-machine system provide several benefits on the model of OMIB which only utilizes a small matrix size with single column for several components used in equation (4). This is contrary with the multi-machine model which is basically according to large matrix size relatively n × k for several components used in [15]. The calculation load will be exoculated at every distance of computation time. In addition, OMIB has the benefit in offering a value of which is straight forward hence providing a fast computation compared to the identified all the nth generating units using the multi-machine model.

2.1. CCT Determine From the One Machine Infinite Bus

Practically, according to the two approaches, the CCT, *tc* can be achieved. Firstly, it is identified before the tested analysis of a system during post-fault situation. Secondly, OMIB equivalent system is used to identify the CCT according to the EAC [16] of the machine given in (15). Technically, the calculation of CCT include an inherent mathematical development deduced from the pre-fault, during fault and post-fault situations [17].

$$t_c = \sqrt{\frac{2H(\delta_c - \delta^o)}{\pi f_{rated} P_m}} \tag{15}$$

where,

δ_c : critical clearing angle

Transient instability is cause by a three-phase fault happened at the bus bar nearest to the substation connected with a sensitive generator, the value of CCT becomes significantly less. It is acceptable to maintain the transient stability even though fault happened at the other locations by setting the protection relay with the obtained value of CCT. A circuit breaker which is functioning earlier than the smallest CCT will not affect to a transient instability during the occurrence of fault.

Assuming that P_m is a fix and it is process stably while transfer power to the system with OMIB rotor angle, δ^0_{OMIB}. The faulted line will be isolated by the circuit breakers during a fault happened at the transfer end of an interconnected link. Elimination of the faulted line will cause the power flowing through the adjacent interconnected link will become double amount. Thus, tripping of the burdened and faulted interconnected link s will delay sending of power from the generator to the infinite bus. Since the resistance of the system is ignored, P_e is equal to zero. The swing equation given in equation (3) becomes equation (16) during the period of fault.

$$\frac{d^2\delta_{OMIB}}{dt^2} = \frac{\pi f_{rated}}{M}\left(P_{m_{OMIB}}\right) \tag{16}$$

By execution the double integration at both sides of (16), it will become

$$\delta_{OMIB} = \frac{\pi f_{rated}}{2M} P_{m_{OMIB}} t c^2_{OMIB} + \delta^0_{OMIB} \tag{17}$$

For that reason, the OMIB CCT, $t_{c_{OMIB}}$ can be achieved from equation (18).

$$t_{c_{OMIB}} = \sqrt{\frac{2M\left(\delta_{Crit_{OMIB}} - \delta^0_{OMIB}\right)}{\pi f_{rated} P_{m_{OMIB}}}} \tag{18}$$

Where, δ_{OMIB} presently defined as the critical clearing angle, $\delta_{Crit_{OMIB}}$, is specified in (19). The M, $P_{m_{OMIB}}$, $P_{max_{OMIB}}$ and δ^0_{OMIB} are achieved by using (2), (4a), (4c) and (9), respectively.

$$\delta_{Crit_{OMIB}} = \frac{P_{m_{OMIB}}}{P_{max_{OMIB}}}\left(\delta_{max_{OMIB}} - \delta^0_{OMIB}\right) + cos\delta_{max_{OMIB}} \tag{19}$$

where,

$$\delta_{max_{OMIB}} = 180^o - \delta^0_{OMIB} \tag{20}$$

Fig. 1 shows the flowchart of overall algorithm of CCT by using OMIB.

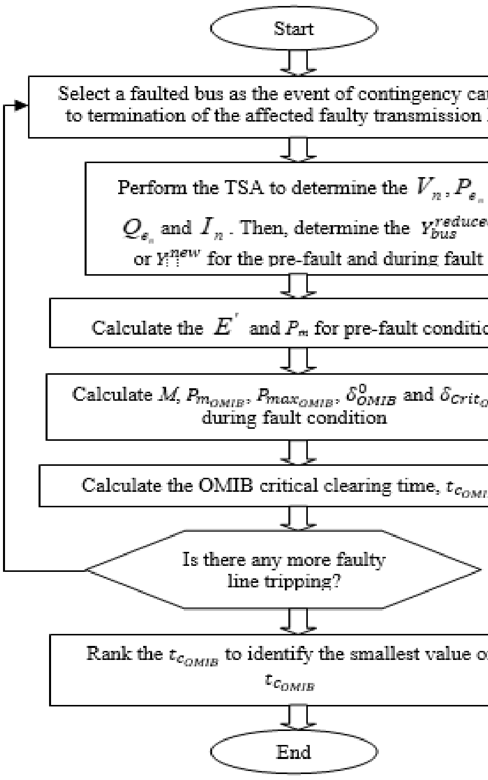

Fig. 1: Flowchart of overall algorithm of CCT by using OMIB.

3. Results and Discussion

This section will explain in detail on the findings of OMIB CCT that is obtained due to the tripping line event of certain faulted line distressed to the IEEE RTS-79 system. The increasing load for each faulted line are 130%, 140% and 150%. In addition, there are 3 types of case study that have been tested which are tripping on generator bus to generator bus, generator bus to load bus and load bus to load bus. The result also showed that the increased of loads will affect the CCT, in other words, the higher the load increasing, the faster the CCT will be obtained. Before obtaining the CCT, there is some process need to be cleared that is the critical clearing angle and the EAC.

Refer to the formula mentioned in the earlier part, to obtain the CCT, critical clearing angle must be obtained first from the EAC. In other word, there is relationship between CCT and critical clearing angle. The lower the critical clearing angle, the shortest CCT will be achieved. The CCT is defined as the maximum allowable time set at a certain protection relay prior to tripping event of interconnected link that contributing to system fault.

Table I shows the result of OMIB CCT that is obtained due to interconnected link tripping event of certain faulted line distressed to the IEEE RTS-79 system. The results have shown that the maximum and minimum CCT of OMIB that is 0.147 second and 0.065 second, respectively are gained in junction to the tripping of faulted lines and increasing load at the faulted lines. For the faulted line and faulted bus that does not contribute to the results of critical clearing angle and CCT, this means that the system can still maintain its stability even though interconnected link tripping occurs.

Table 1: Overall Result of CCT, t_c For Each Faulted Bus At 130% Total Loading Increment

Faulted Line		Faulted Bus	$\delta_{c_{OMIB}}$ (°)	$t_c(s)$	Faulted Line		Faulted Bus	$\delta_{c_{OMIB}}$ (°)	$t_c(s)$	Faulted Line		Faulted Bus	$\delta_{c_{OMIB}}$ (°)	$t_c(s)$
From Line	To Line				From Line	To Line				From Line	To Line			
1	2	1	N/A	N/A	8	9	8	N/A	N/A	14	16	14	101.91	0.131
1	2	2	N/A	N/A	8	9	9	N/A	N/A	14	16	16	71.18	0.088
1	3	1	N/A	N/A	8	10	8	N/A	N/A	15	16	15	59.97	0.065
1	3	3	N/A	N/A	8	10	10	N/A	N/A	15	16	16	65.20	0.077
1	5	1	N/A	N/A	9	11	9	N/A	N/A	15	21	15	64.93	0.076
1	5	5	N/A	N/A	9	11	11	115.97	0.147	15	21	21	76.25	0.096
2	4	2	N/A	N/A	9	12	9	N/A	N/A	15	24	15	65.69	0.077
2	4	4	N/A	N/A	9	12	12	N/A	N/A	15	24	24	105.64	0.135
2	6	2	N/A	N/A	10	11	10	N/A	N/A	16	19	16	65.87	0.078
2	6	6	N/A	N/A	10	11	11	115.77	0.146	16	19	19	79.29	0.101
3	9	3	N/A	N/A	10	12	10	N/A	N/A	17	18	17	81.66	0.105
3	9	9	N/A	N/A	10	12	12	N/A	N/A	17	18	18	81.34	0.104
3	24	3	N/A	N/A	11	13	11	114.68	0.145	17	22	17	81.00	0.104
3	24	24	N/A	N/A	11	13	13	115.75	0.146	17	22	22	106.48	0.136
4	9	4	N/A	N/A	11	14	11	114.20	0.145	18	21	18	81.34	0.104
4	9	9	N/A	N/A	11	14	14	100.89	0.130	18	21	21	76.62	0.097
5	10	5	N/A	N/A	12	13	12	N/A	N/A	19	20	19	85.90	0.111
5	10	10	N/A	N/A	12	13	13	116.57	0.147	19	20	20	93.66	0.121
6	10	6	N/A	N/A	12	23	12	N/A	N/A	20	23	20	94.16	0.122
6	10	10	N/A	N/A	12	23	23	96.61	0.125	20	23	23	95.93	0.124
7	8	7	N/A	N/A	13	23	13	116.64	0.147	21	22	21	75.93	0.096
7	8	8	N/A	N/A	13	23	23	96.53	0.125	21	22	22	106.41	0.136

Fig. 2 and Fig. 3 shows the result of CCT for faulted bus number 13 and 23 and the load was increased at 130%, 140% and 150% of its total loading increment. In Fig. 2, bus 13 was selected as the faulted bus, nevertheless, in Fig. 3, the faulted bus was selected to be bus 23. In this case the tripping line is the connection between generator bus to generator bus. The graph showed the result for the EAC after applying the OMIB method and the critical clearing angle and CCT can be obtained. P_m in the graph represents the mechanical power and the blue and pink colour represents the electrical power, P_e. The area of shaded region for pink represents the kinetic energy stored by the rotor during acceleration, and the area of shaded region for blue represents the kinetic energy given up by the rotor to the system, and when it is all given up, the generator has returned to its synchronous speed. The areas under the curve should be zero for both areas, which is possible only when both have decelerating and accelerating powers, for example for a part of the curve $P_e > P_m$ and for the other $P_m > P_e$. For a generation action, $P_e > P_m$ for negative area (blue) and $P_m > P_e$ for the positive area (pink) for stable operation.

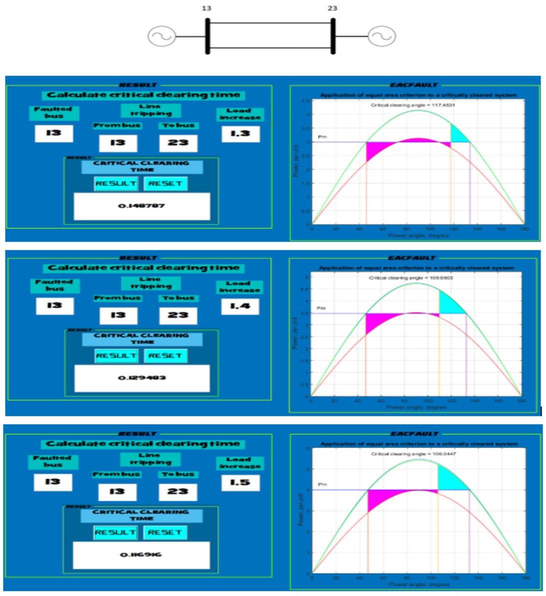

Fig. 2: Interconnected link [13 23] and bus 13 trip

That is why it call as EAC. The function of EAC is to determine the maximum limit on the load that the system can take without exceeding the stability limit. This can happen only when the area between the P_e curve and the P_m line is equal to the area between the P_e curve and P_m line is equal to the area between the primary torque angle and the line P_m. In this case, the area of shaded region for pink and blue is not equal, so the system will become unstable. This result also showed that the higher the load increase the shorter the time required to clear the fault.

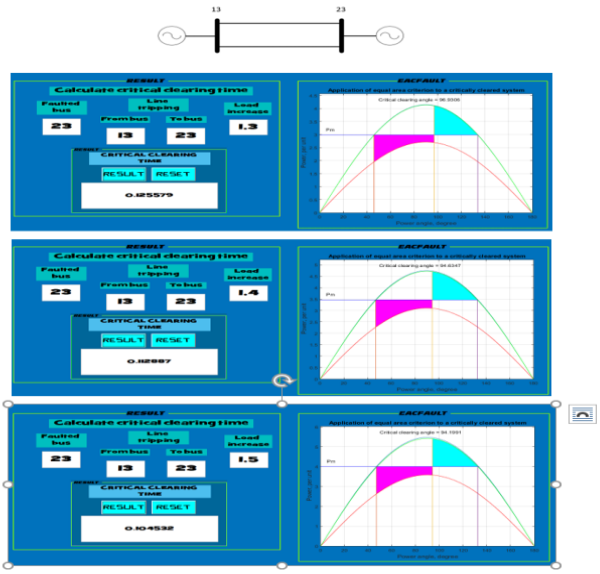

Fig. 3: Interconnected link [13 23] and bus 23 trip

Figure 4 and Figure 5 shows the result of CCT for faulted bus number 20 and 23 and the load was increased. Figure 4 selects bus 20 as the faulted bus, nevertheless Figure 5 choose bus 23 as the faulted bus. In this case the tripping line is the connection between load bus ang generator bus. The EAC was achieved and same with the previous result. This EAC method has been explained and discuss from the previous table of result. In this case, the area of shaded region for pink and blue is not equal, so the system will become unstable. This result also showed that the higher the load increase the shorter the time required to clear the fault.

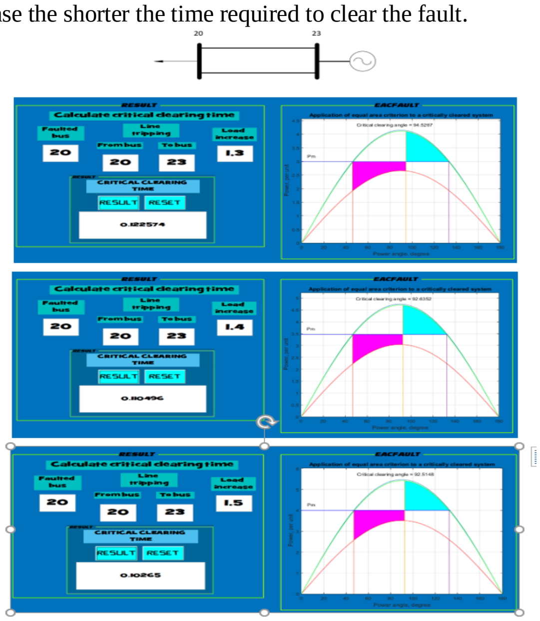

Fig. 4: Interconnected link [20 23] and bus 20 trip

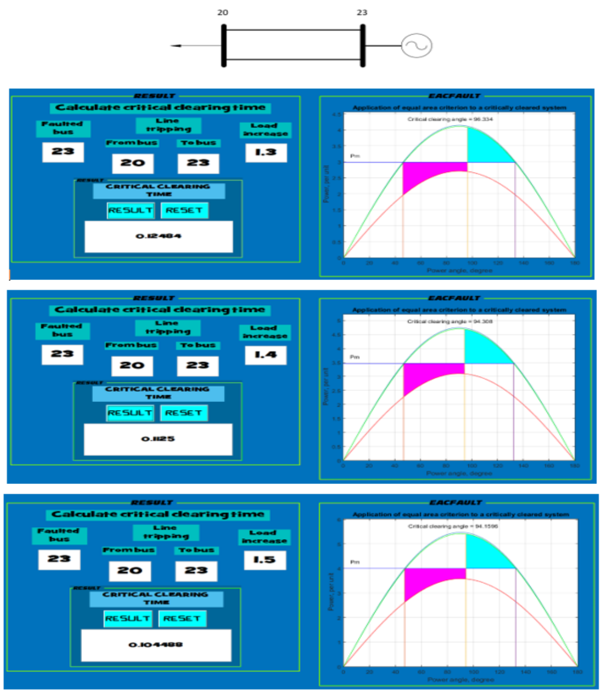

Fig. 5: Interconnected link [20 23] and bus 23 trip

Fig. 6 and Fig. 7 shows the result of CCT for faulted bus number 19 and 20 and the load was increased. Fig. 6 selects bus 19 as the faulted bus, nevertheless Fig. 7 choose bus 20 as the faulted bus. In this case the tripping line is the connection between load bus to load bus. The EAC was achieved and same with the previous result. This EAC method has been explained and discuss from the previous table of result. In this case, the area of shaded region for pink and blue is not equal, so the system will become unstable. This result also showed that the higher the load increase the shorter the time required to clear the fault.

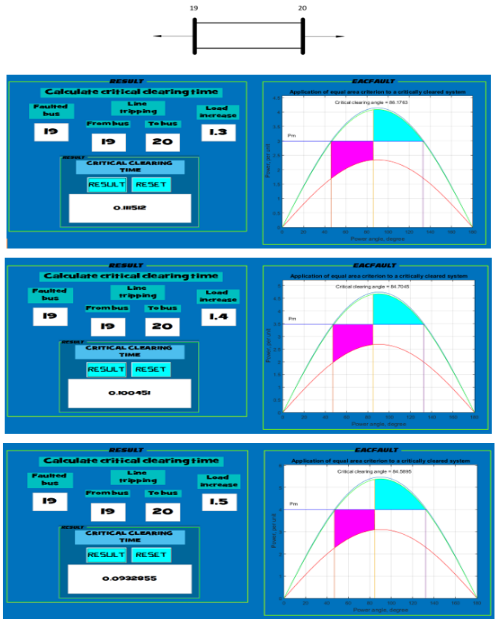

Fig. 6: Interconnected link [19 20] and bus 19 trip

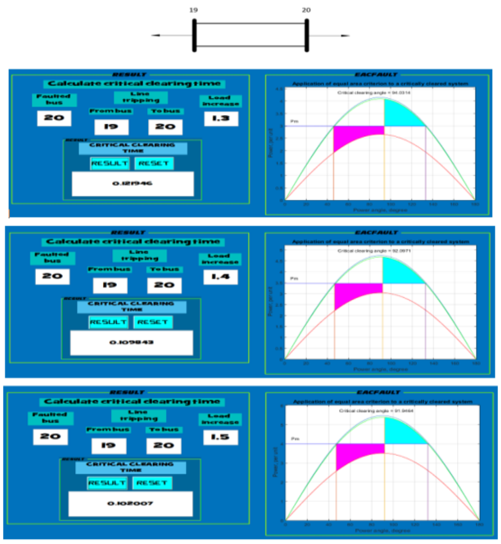

Fig. 7: Faulted bus 20 trip line [19 20]

4. Conclusion

Disconnection of an interconnected link during the event of contingency event in an electricity supply is performed to insulate the fault from an excellent system. For that reason, by disconnecting the interconnected link at inappropriate time is not very encouraged because it will cause the generator to face the loss of synchronism which can affect the transient stability of a system. For that reason, to make the system transiently remains stable, the transient stability analysis must be performed so that the suitable CCT for line tripping can be obtained. Thus, to avert any breakdown or a generator experience the loss of synchronism, the process of a protection relay should be set referring to the CCT so that the fault can be cleared. Furthermore, by solving the swing equation in the EAC method, specified CCT can be obtained that subjected to the system response upon line tripping. The EAC is a simple graphical method for concluding the transient stability of a single machine against an infinite bus. The situation of the stability is identified by differentiate the areas of sections on the power angle diagram between the p-curve and the new power transfer line of the given curve. The principle of this technique involves on the basis that when δ oscillates around the equilibrium point with fix amplitude, transient stability will be maintained. For that reason, the CCT for each interconnected link has proven that can be obtained precisely by the proposed technique of OMIB equivalent and the EAC. In order to prevent the electricity supply from any kind of distraction events, the calculation of CCT should be carried out accurately in the electricity supply transient stability analysis. Hence, from the method of OMIB equivalent also can conclude whether the whole system itself is stable or not stable. Last but not least, the implementation of GUI in this research is the easiest way to monitor the CCT.

Acknowledgement

The authors would like to thank the Research Management Institute (RMI), Universiti Teknologi MARA, Malaysia and the Ministry of Higher Education (MOHE), Malaysia through research grant 600-IRMI/DANA 5/3/BESTARI (121/2018) for the financial support of this research.

References

[1] M. Venkatasubramanian and K. Tomsovic, Electricity supply Analysis. WCB/McGraw-Hill, 2005.

[2] G. R. Walke, "Improving Transient Stability ofElectricity supply by using Distributed Static Series Compensator," 2016.

[3] N. A. Salim, M. M. Othman, M. S. Serwan, and S. Busan, "a Single Machine Equivalent Approach for the Amelioration of CCT Limit," vol. 10, no. 19, pp. 8972–8979, 2015.

[4] P. G. Pavella, M. ; Murthy, Transient stability of electricity supplys: Theory and practice. New York, NY (United States); John Wiley and Sons.

[5] N. A. Salim, M. M. Othman, I. Musirin, and M. S. Serwan, "The Impact of System Sequence of fault and Interconnected link Outages to the Transfer Capability Assessment," vol. 8, no. 2, pp. 250–253, 2014.

[6] S. Ayasun, Y. Liang, and C. O. Nwankpa, "A sensitivity approach for computation of the probability density function of CCT and probability of stability in electricity supply transient stability analysis," Appl. Math. Comput., vol. 176, no. 2, pp. 563–576, 2006.

[7] H.-D. Chiang, F. F. Wu, and P. P. Varaiya, "Foundations of the potential energy boundary surface method for electricity supply transient stability analysis," IEEE Trans. Circuits Syst., vol. 35, no. 6, pp. 712–728, 1988.

[8] H. Chiang, F. F. F. F. Wu, P. P. P. Varaiya, H. Chiang, F. F. F. F. Wu, and P. P. P. Varaiya, "A BCU method for direct analysis of electricity supply transient stability," IEEE Trans. Power Syst., vol. 9, no. 3, pp. 1194–1208, 1994.

[9] Y. Xue, T. Van Cutsem, and M. Ribbens-Pavella, "Extended EAC justifications, generalizations, applications," IEEE Trans. Power Syst., vol. 4, no. 1, pp. 44–52, 1989.

[10] A. A. Fouad and V. Vittal, Electricity supply transient stability analysis using the transient energy function method. Pearson Education, 1992.

[11] D. Z. Fang and A. K. David, "A normalized energy function for fast transient stability assessment," Electr. Power Syst. Res., vol. 69, no. 2–3, pp. 287–293, 2004.

[12] S. Busan, "Dynamic Available Transfer Capability Calculation Considering Generation Rescheduling," Master Sci. Electr. Eng. Univ. Teknol. MARA, 2012.

[13] M. M. Othman, S. Busan, I. Musirin, A. Mohamed, and A. Hussain, "A new algorithm for the available transfer capability determination," Math. Probl. Eng., vol. 2010, 2010.

[14] M. Pavella, D. Ernst, and D. Ruiz-Vega, "Transient Stability of Electricity supplys A Unified Approach to Assessment and Control," Kluwer Acad. Publ., pp. 1–254, 2000.

[15] D. Layden, Transient Stability Assessment and Preventive Control of Electricity supplys. Library and Archives Canada= Bibliothèque et Archives Canada, 2006.

[16] R. Zarate-Minano, T. Van Cutsem, F. Milano, and A. J. Conejo, "Securing Transient Stability Using Time-Domain Simulations Within an Optimal Power Flow," IEEE Trans. Power Syst., vol. 25, no. 1, pp. 243–253, 2010.

[17] B. Boussahoua and M. Boudour, "CCT evaluation of electricity supply with UPFC by energetic method," J. Electr. Syst., vol. 5, no. SUPPL. 1, pp. 85–88, 2009.

[18] G. Srinivasulu, "Multi- Objective Transmission Expansion Planning for IEEE 24 Bus RTS," pp. 144–149, 2015.